NATURE, PROPORTION AND DISTRIBUTION OF STACKING FAULTS IN CELADONITE MINERALS

F. Muller[1], A. Plançon[1] , G. Besson[1] and V. A. Drits[2]

[1]Centre de Recherche sur la Matière Divisée, U.M.R. Université d'Orléans - C.N.R.S., B.P. 6759, rue de Chartres, 45067 Orléans Cedex 2, France

[2]Geological Institute, Russian Academy of Sciences, Pyzhevskii Street 7, 109017 Moscow, Russia

Abstract

Selected area electron diffraction (SAED) and X-ray accurate measurement of the basal distance of celadonite have not confirmed stacking faults different from $n \times 60°$ rotations (n-integer). Two models for stacks containing defects can be imagined differing by the range R of the interactions between layers. If the orientation of a layer depends on the orientation of the preceding one, $R = 1$, else $R = 0$. The calculated XRD patterns for these two structural models are almost identical. In order to clear up the ambiguity celadonite samples have been heated to 650 °C and studied by SAED. At this temperature, a dehydroxylation reaction accompanied by an octahedral cations migration from *cis*- into *trans*-sites transforms the *C*-centered layer unit-cell into a primitive one. The SAED pattern of the heated sample exhibit *hk*0 reflections distributed according a single primitive unit-cell which excludes a stack of layers with $R = 1$.

1. Introduction

Celadonites are dioctahedral 2:1 phyllosilicates of structural formula [1]:

K_{x+y} $(Mg, Fe^{II})_x(Al, Fe^{III})_{2-x}$ $Si_{4-y}(Al, Fe^{III})_y$ $O_{10}(OH)_2$

where K^+ is the interlayer cation which compensates the negative charge of the layer arising from cation substitutions inside the layer. The 2:1 notation means that layers are formed of two sheets of tetrahedra sandwiching a sheet of octahedra. Dioctahedral means that in the octahedral sheet, only two of the three sites per one half unit-cell are occupied. The nature of the octahedral cations varies in the 2:1 dioctahedral phyllosilicates family, the celadonites being Fe^{3+}-rich. The vacant site can be in a *trans* position (*tv* layer, *C12/m(1)* space-group) or in one of the two *cis* positions (*cv*1 or *cv*2 layer, *C12(1)* space-group, Figure 1). Structural studies have shown that natural celadonites are built of *tv* layers [2-4] as presented in Figure 1.

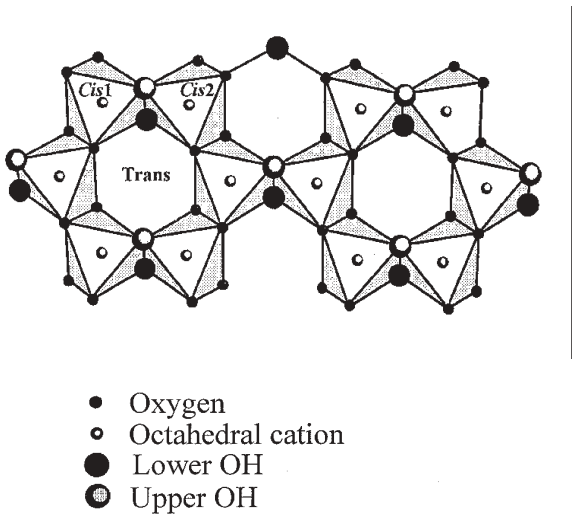

Figure 1: Schematical representation of the octahedral sheet in the case of *tv* layers

It is well know that the stacking of the layers in phyllosilicates is rarely perfect. Depending on the phyllosilicate it can contain random translational or rotational stacking faults (e.g. smectites [5]), or well defined translational defects (such $\pm b/3$ e.g. kaolinites [6]) or well defined rotations by $n \times 60°$ (e.g. glauconites [7]). Whatever the nature of the stacking faults they always produce in XRD powder patterns: (i) a raising of the background between reflections and (ii) a broadening of some families of reflections (or all of them) [8]. For example, Figure 2 shows the calculated XRD powder pattern for celadonite (a) without stacking faults, (b) with a 0.10 probablity of $n \times 60°$ rotational stacking fault in a model with $R = 0$ (see below the explanation of R) and (*c*) with a 0.15 probability of such rotational stacking faults. The existence in the experimental patterns (Figure 4) of a non negligible background between reflections and the rather large width of all reflections indicates that the natural samples contain stacking faults. One goal is to clarify their nature.

Independently on the nature of the stacking faults we have to keep in mind that their distribution also must be precised. In fact there are two models which differ by the range of the interaction between layers (the reichweite, R, introduced by Jagodzinski [9]). If $R = 1$ the orientation of a layer in a given coherent scattering domain depends on the orientation of the preceding one i.e. after a rotation stacking fault the layer stacks preferentially with the orientation of the rotated layer (Fig. 3); on the contrary for $R = 0$ it stacks independently of the orientation of this layer. Usually the most efficient method for the determination of nature, proportion and distribution of the stacking faults in powder materials is the X-ray diffraction. Therefore, this method has been used for the characterization of faults in celadonite. Another efficient method is the selected area electron diffraction (SAED). Two layers rotated by an α angle will produce in SAED patterns two sets of reflections rotated by the same angle.

We will now show the results obtained by these two diffraction techniques.

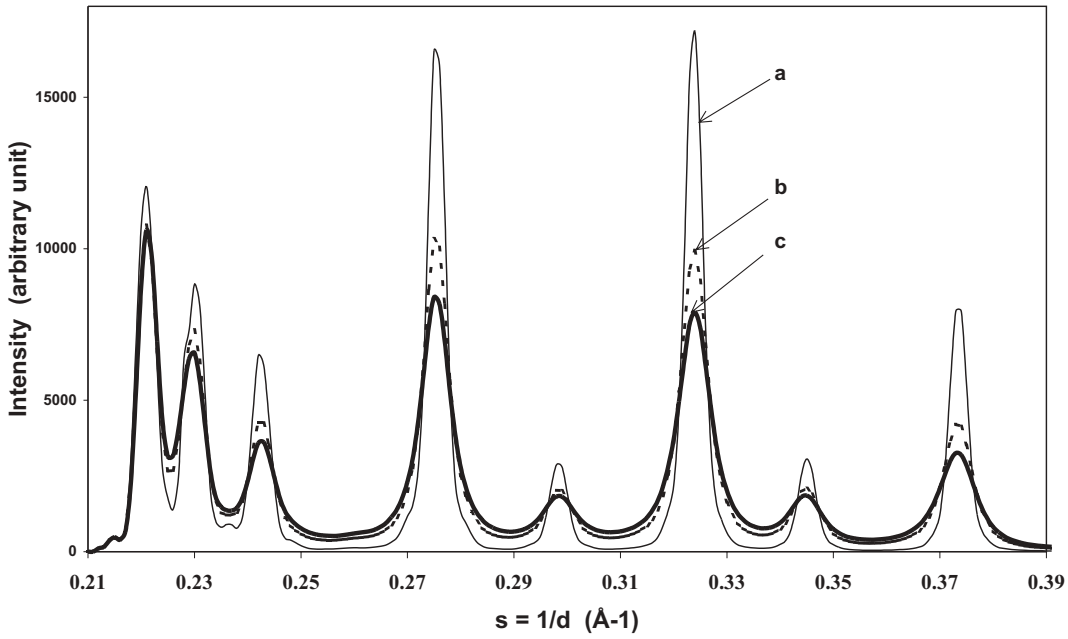

Figure 2. Calculated XRD powder patterns for celadonite (a) without stacking faults, (b) with a 0.10 probability of rotational stacking fault in a model with R = 0 and (c) with a 0.15 probability of rotational stacking fault R = 0)

2. Experimental

The chemical composition of the celadonite sample of Pobuzhyie (Russia) [10] used in this study is given in Table 1. It corresponds to typical celadonite after nomenclature of the micas [1] because:

$(Mg + {}^{VI}Fe^{II}) / (Mg + {}^{VI}Fe^{II} + {}^{VI}Al + {}^{VI}Fe^{III}) = 0.49$, i.e. > 0.25.
${}^{VI}Al / ({}^{VI}Al + {}^{VI}Fe^{III}) = 0.05$, i.e. < 0.5.
$Mg / (Mg + {}^{VI}Fe^{II}) = 0.74$, i.e. > 0.5.

Table 1. Cation composition of the sample under study per $O_{10}(OH)_2$ [10]

Tetrahedral cations		Octahedral cations				Interlayer cations	
Si	^{IV}Al	^{VI}Al	^{VI}Fe^{III}	^{VI}Fe^{II}	Mg	K	Ca
3.96	0.04	0.05	0.96	0.26	0.73	0.89	0.10

2.1 XRD Data

The powder XRD patterns have been recorded in transmission and reflection geometry. Transmission experiments have been done using MoKα radiation (λ = 0.70926 Å), with a diffractometer supplied with a curved position-sensitive detector INEL CPS 120. The sample holder was a 1mm-diameter silica-glass tube that provides a disordered orientation of the particles inside. Recordings were made for 02*l*, 11*l*, 20*l* and 13*l* reflections which are most sensitive to site occupancy and the nature of stacking faults.

In reflection geometry (Siemens D500, CuKα radiation, λ= 1.5418 Å), an oriented sample was prepared in order to determine precisely the basal distance d_{001} from the d-spacing of several 00 reflections.

2.2 SAED *Data*

The sample has been studied in its natural state and after heating from room temperature to 700 °C with a step of 50 °C and a heating rate of 100 °C/hour. At each step the temperature was maintained for 1 hour and the sample was then cooled in air. After ultrasonic treatment, sample suspensions were dropped onto carbon grids. SAED patterns were recorded using a JEOL-100cx microscope equipped with a tilting sample holder and operated at 100 kV.

3. Nature of the stacking faults

The different stacking faults found in phyllosilicates and mentioned above have been considered for celadonite i.e. random translational or rotational stacking faults and/or well defined translational faults (by ± *a*/3, ± *b*/3, ± *a*/3 ± *b*/3 for example). The determination of the parameters of the unit-cell of celadonite (a = 5.21 ± 0.01 Å, b = 9.060 ± 0.005 Å, c = 10.20 ± 0.01 Å and β = 100.7 0.1°) using XRD shows that in the mean stacking two adjacent layers are positioned such a way that the ditrigonal cavities of their tetrahedral sheets [11] face each other, the K^+ cation being located in these cavities and anchoring these adjacent layers. The strength of this anchoring is sufficient to prevent any swelling of the interlayer space whatever nature of the solvating molecule [12].

SAED experiments which were performed (Figure 5a) show that there are no random rotational stacking faults, because patterns for single-particles do not display the superposition of rotated sets of reflections.

In addition, random stacking faults, as well as well defined translational ones should result in an increase of the interlayer distance, because K^+ cation would not be engaged on both sides into the ditrigonal cavities of the tetrahedral sheets. Careful measurements by XRD of the 00*l* *d*-spacings of the natural sample have led to a basal distance $d_{001} = 9.98 \pm 0.01$ Å which is exactly the d_{001} of micas which are 2 : 1 dioctahedral phyllosilicate with K as interlayer cation and which are defect free [13]. A 10% proportion of 11 Å layers should led to a 10.1 Å d-spacing (11 Å should correspond to a stacking in which K is engaged in ditrigonal cavities only one on side; a stacking in which K will face oxygen atoms in both sides should lead to a 12.0 Å spacing, assuming a 1.40 Å ionic radius for oxygen and 1.33 Å ionic radius for potassium).

So the first conclusion based on crystallochemical considerations and on observation in SAED or measurements in XRD is that the faults in celadonite can be only $n \times 60°$ rotations defects.

4. Distribution and proportion of stacking faults

4.1 Powder XRD simulation

For the natural sample consisting of tv 2:1 layers the atomic coordinates were calculated by the Smoliar-Zviagina's method [14] which uses experimentally determined data i.e. chemical composition (Table 1) and unit-cell parameters (Table 2). Table 3 contains these calculated atomic coordinates along with the sites occupancies.

Table 2. Unit-cell parameters calculated from the peak positions of the XRD patterns.

a(Å)	b(Å)	c(Å)	β(°)
5.21±0.01	9.060±0.005	10.20±0.01	100.7±0.1

XRD patterns were simulated with the program CALCIPOW based on the description of the powder diffracted intensities of one-dimensionally disordered structures by a matrix formalism [15-17]. Each azimuthal layer orientation was considered as a layer type. Coherent scattering domains (CSD) in the layer plane were assumed as having disk-like shape with a mean radius found by fitting reflections with $l = 0$.

In case of $R = 0$ one of the six possible orientations of layers prevails with an abundance W_0. The abundances W_i of the 5 other possible orientations by $n \times 60°$ were considered as equally distributed. Then $W_{60} = W_{120} = ... = W_{300} = (1\text{-}W_0)/5$. If W_0 is significantly higher than $\sum_{n=1}^{5} W_{nx60}$, then the distribution of stacking faults may be represented schematically as in Figure 3a.

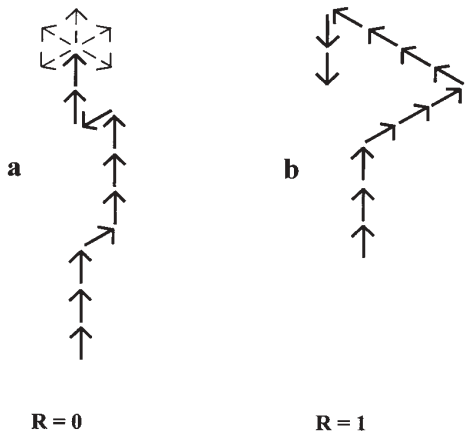

Figure 3. Schematical representations of the distribution of $n \times 60°$ stacking faults for (a) $R = 0$ and (b) $R = 1$

Table 3. Atomic coordinates, site occupancies and structural parameters used for XRD pattern simulations calculated from data of Tables 1 and 2 using Smoliar-Zviagina's formulas [14]

		Atomic coordinate				Site occupancy
		x/a	y/b	z/c sin β	z(Å)	
Oxygens		0.633	0.316	0.611	6.124	2
		0.633	0.684	0.611	6.124	2
		0.648	0.500	0.828	8.299	2
		0.880	0.245	0.833	8.349	2
		0.880	0.755	0.833	8.349	2
		0.008	0.316	0.388	3.889	2
		0.008	0.684	0.388	3.889	2
		0.993	0.500	0.172	1.724	2
		0.761	0.245	0.167	1.674	2
		0.761	0.755	0.167	1.674	2
Hydroxyls		0.688	0.000	0.611	6.124	2
		0.953	0.000	0.389	3.899	2
Tetrahedral cations		0.636	0.332	0.771	7.727	1.98Si+ 0.02Al
		0.636	0.668	0.771	7.727	1.98Si+ 0.02Al
		0.005	0.332	0.229	2.295	1.98Si+ 0.02Al
		0.005	0.668	0.229	2.295	1.98Si+ 0.02Al
Octahedral cations	Al	0.320	0.667	0.5	5.011	0.05
		0.320	0.333	0.5	5.011	0.05
	Mg	0.320	0.667	0.5	5.011	0.73
		0.320	0.320	0.5	5.011	0.73
	Fe	0.320	0.667	0.5	5.011	1.22
		0.320	0.320	0.5	5.011	1.22

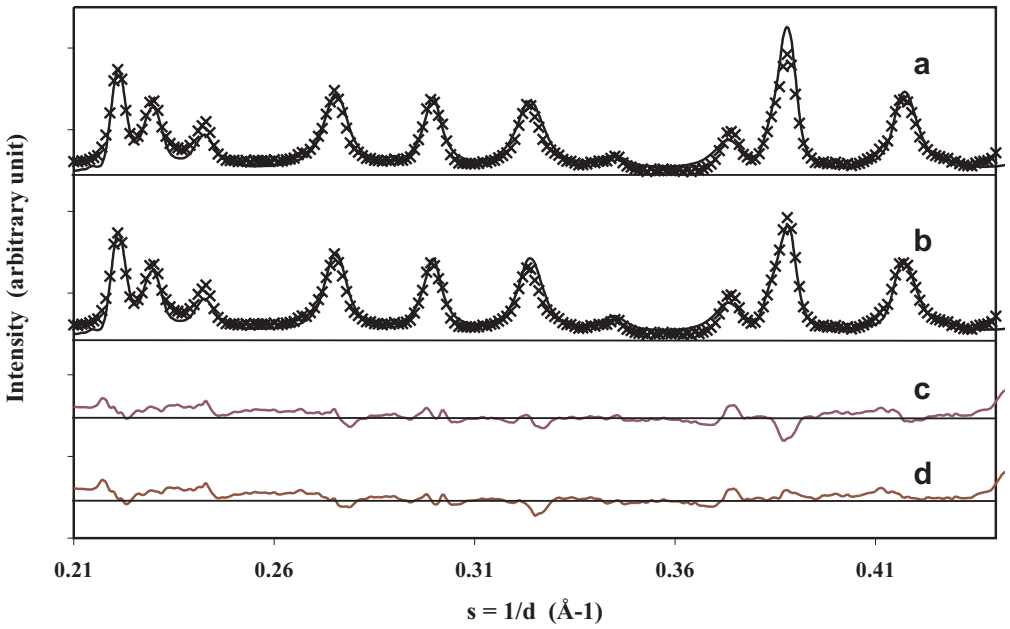

Figure 4. XRD patterns at room temperature and their computer simulation with (a) $R = 0$ and (b) $R = 1$ (solid line : calculated pattern; crosses : experimental pattern). Difference between calculated an observed intensities for model with (c) $R = 0$ and (d) $R = 1$

CDS (Å)	Structural parameter
	125
No of layers	25

In case of $R = 1$, all orientations of layers are equally probable, that is, $W_0 = W_{60} = ... = W_{300} = 1/6$. Then a set of junction probabilities P_{ij} should be added to calculate the occurrence probabilities for layer sub-sequences (P_{ij} is the junction probability that a layer of type j follows a layer type i). If layers of a given orientation are distributed with some degree of segregation the junction coefficients P_{ii} are such that $W_i < P_{ii} \leq 1$ (i = 0, 60°,120°, 180°, 240°, 300°) This corresponds to the sketch of Figure 3b.

Figure 4 is a comparison of the experimental XRD pattern of natural celadonite with calculated ones corresponding to the two models of stacking with rotational nx60° faults. The conclusion is that patterns for both models are in a good agreement with the experimental XRD curves. For $R = 0$ the best fit is obtained with $W_0 = 0.85$, while for $R = 1$ it is with $W_i = 0.167$ and $P_{ii} = 0.75$. So the X-ray diffraction does not identify the distribution of the rotational stacking defects in celadonite.

4.2 SAED results

SAED experiments show that there is no change between room temperature and 600 °C. Changes occur at 650 °C and beyond. Due to the difficulty to achieve a complete separation of the crystals the SAED patterns will unfortunately correspond to the contribution of several superposed crystals in the diffracting zone.

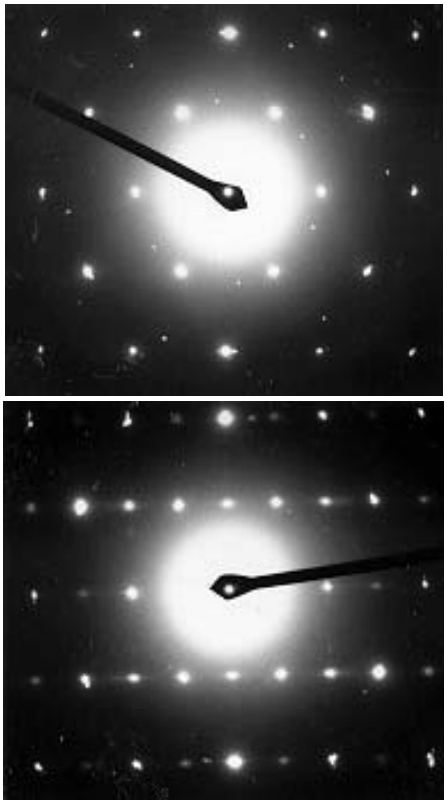

Figure 5. SAED patterns at room temperature (top) and after heating at 650°C (bottom)

- SAED on natural celadonite samples : A thick crystal and a thinnest one, rotated by 22° contribute to SAED. For each crystal the pattern can be described by a set of strong $hk0$ reflections whose positions are distributed according an

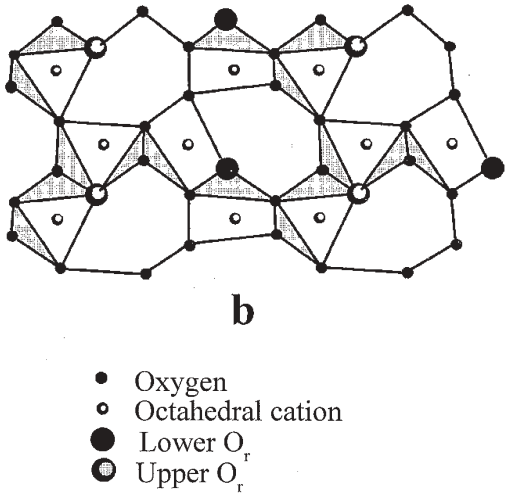

Figure 6. Schematical representation of the octahedral sheet for the *cv* dehydroxylated celadonite [19]

hexagonal symmetry. For individual layers the reciprocal space is constituted of *hk* rods, normal to the layer plane; their positions have an hexagonal symmetry because i) $b = a\sqrt{3}$ and ii) there are only $h + k = 2n$ reflections for a *C*-centered unit-cell. The diffracted patterns of the crystals show also this symmetry meaning that layers inside crystals can be rotated only by $n \times 60°$.

- SAED on 650 °C heated celadonite sample : there is no change in the morphological features of the particles. For the same reasons as previously the SAED pattern shown on this figure contains reflections of a second crystal, rotated respectively the first one by 7°. The SAED patterns of single crystals remain fundamentally the same as room temperature ones except that additional reflections arise with $h+k \neq 2n$ (Figure 5b). The distribution of the *hk*0 reflections in this pattern can be described by a primitive unit-cell with $a = 5.23 \pm 0.01$ Å, $b = 9.06 \pm 0.01$ Å and $\gamma = 90.0 \pm 0.1°$.

- SAED on 650 °C heated celadonite sample : there is no change in the morphological features of the particles. The SAED patterns of single crystals remain fundamentally the same as room temperature ones except that additional reflections arise with $h+k \neq 2n$ (Figure 5b). The distribution of the hk0 reflections in these pattern can be described by a primitive unit-cell with $a = 5.23 \pm 0.01$ Å, $b = 9.06 \pm 0.01$ Å and $\gamma = 90.0 \pm 0.1°$.

- SAED on 700 °C and 750 °C heated celadonite sample : the observation of particles shows that they have been broken up. In SAED broad diffraction rings appear while reflections themselves vanish.

Between room temperature and 650 °C the framework of the layers is kept and the dehydroxylation process induces, except the replacement of 2 OH groups by an oxygen atom, limited reorganization of the atoms resulting in the transformation of the C centered unit cell into a primitive one. The strong anchorage of the layers through the K^+ interlayer cation prevent a reorganisation of the stacking of the layers. Beyond 650 °C a strongest reorganisation of the atoms occurs with the transformation of the celadonite into spinel [18].

The origin of the primitive unit-cell is as follows. Around 650 °C, the dehydroxylation process occurs [19], corresponding to the replacement of two adjacent hydroxyl groups by a residual oxygen atom O_r according to the reaction: $2(OH) \rightarrow H_2O(\uparrow) + O_r$. The water molecule migrates out of the structure. X-ray powder diffraction [19] and oblique texture electron diffraction [20] show that the octahedral cations migrate from *cis*- into *trans*-sites in the dehydroxylated celadonites, transforming the *C*-centred

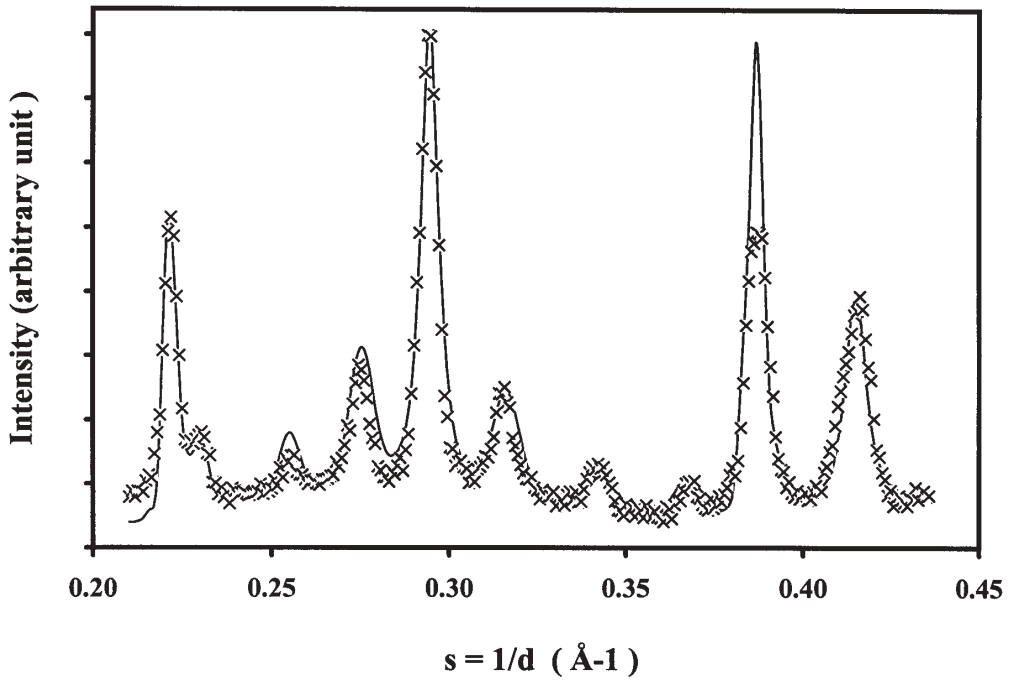

Figure 7. XRD pattern at 650°C and the computer simulation for the sample [15]

layer unit-cell into a primitive one [19]. Figure 6 shows the schematic representation of the octahedral sheet in the of *cv* dehydroxylated celadonites which has been deduced from a comparison of the XRD pattern of celadonite heated to 650 °C with calculated ones (Figure 7).

Let us recall figures 1 and 6 depict only the octahedral sheets of the layers. Octahedral sheets are sandwiched between two tetrahedral sheets which are only slightly affected by the migration of the octahedral cations. The stacking itself of the layers which depends fundamentally on the tetrahedral sheets of the adjacent layers facing each other and is almost unaffected by the octahedral cation migration.

What should be the SAED pattern in case of $n \times 60°$ rotational stacking defects with a $R = 1$ distribution ? For sufficiently thick crystals (SAED patterns are taken on crystals more than 25 layers thick) with a 0.25 probability of stacking defects between adjacent layers (determined by XRD), all 6 equally probable orientations should contribute to the SAED pattern. That is, this pattern should exhibit 3 primitive unit cells (layers related by a 180° rotation lead to the same unit cell) with approximately the same intensities. This does not correspond to the observations.

On the contrary, one orientation dominates if $R = 0$. From XRD results, for $R = 0$, $W_0 = 0.85$, $W_{60} = W_{120} = ... = W_{300} = 0.15/5$. Thus 88% of the layers contribute to the intensity of the predominant unit-cell in the SAED pattern. The absence in SAED diagram of the weak rotated primitive unit-cells which nevertheless could be expected from the small proportion of the other layers probably owes its origin to the fact that each of these orientation is 15 times less probable, leading to a factor about 200 in intensities ratios.

5. Conclusions

The existence in the XRD patterns of celadonite of a non negligible background between reflection and a rather important width of the reflections indicates that these minerals contain layer stacking faults. Random stacking faults (by rotation or translation) as well as well-defined translational faults are not only difficult to understand from a crystallochemical point of view but are also excluded by accurate measurements of the basal distance d_{001}. Rotational stacking faults by $n \times 60°$ (n integer) are compatible with the SAED patterns. The calculation of theoretical XRD patterns show that the two models with a distribution of their faults with an interaction range $R = 0$ or $R = 1$ lead to the same results. SAED performed on dehydroxylated sample shows unambiguously that in the stacking there is a prevailing orientation of layers, that is $R = 0$, with an abundance of defectively oriented layers of 0.15.

References

1. Rieder M., Cavazzini G., D'yakonov Y.S., Frank-Kamenetskii V.A., Gottardi G., Guggenheim S., Koval P.V., Müller G., Neiva A.M.R., Radoslovich E.W., Robert J.L., Sassi F.P., Takeda H., Weiss Z., Wones R.D.: *Clay Clay Miner*., **46** (1998), 586-595.
2. Bookin A.S., Dainyak L.G., Drits V.A.: *Phys. Chem. Minerals,* **3** (1978), 58-59.
3. Tsipursky S.I., Drits V.A., Chekin S.S.: *Izvestiya Akademii Nauk S.S.S.R., Ser. Geol.,* 10 (1978), 105-113 (in Russian).
4. Dainyak L.G., Bookin V.A., Drits V.A.,Tsipursky S.I.: *Acta Crystallogr.,* **A37** (1981), C-362.
5. Besson G.: Doctorat d'état,Orléans University, France, 1980 (in French).
6. Plançon A., Tchoubar C.: *Clay Clay Miner*., **25** (1977), 436-450.
7. Sakharov B.A., Besson G., Drits V.A., Kameneva M. Yu., Salyn A.N., Smoliar B.B.: *Clay Minerals,* **25** (1990), 419-435.
8. Drits V.A., Tchoubar C..X-ray diffraction by disorderer lamellar structures, chap. VIII, Springer-Verlag Berlin Heidelberg, 1990, 233-300.
9. Jagodzinski H.. *Acta Crystallogr.,***2** (1949), 201-207.
10. Malkova K.M.: *Zapiski Lvovskogo Mineralogicheskogo obshestva,* **10** (1956), 305-318 (in Russian).
11. Bailey S. W.: Reviews in mineralogy, volume 13, Micas, chap. 1, S. W. Bailey ed., 1984, 1-12.
12. Odom E.: Reviews in mineralogy, volume 13, Micas, S. W. Bailey ed., 1984, 545-571.
13. Bailey S. W.: Crystal structures of clay minerals and their X-ray identification, G.W. Brindley and G. Brown ed., Mono 5, Mineralogical Soc., London, 1980, 1-124.
14. Smoliar-Zviagina B.B.: *Clay Miner*., **28** (1993), 603-624.
15. Plançon A.: *J. Appl. Crystallogr*., **14** (1981), 300-304.
16. Sakharov B.A., Naumov A.S., Drits V.A., *Doklady* AN SSSR, **265** (1982), 339-343 (in Russian).
17. Sakharov B.A., Naumov A.S., Drits V.A.: *Doklady* AN SSSR, **265** (1982), 871-874 (in Russian).
18. Mackenzie R.C.: The differential thermal investigation of clays, R.C. Mackenzie ed., Mineralogical Soc., London, 1957, 165-190.
19. Muller F., Plançon A, Drits V. A., Besson G.: *J. Phys IV*, **8** (1998), 91-98.
20. Plançon A, Tsipursky S.I., Drits V.A.,: S*ov. Phys. Crystallogr.* **30** (1) (1985), 18-22.